Article

Matrix Isolation, Spectroscopic Characterization, and Photoisomerization of *m*-Xylylene

Patrik Neuhaus, Dirk Grote, and Wolfram Sander

J. Am. Chem. Soc., **2008**, 130 (10), 2993-3000 • DOI: 10.1021/ja073453d

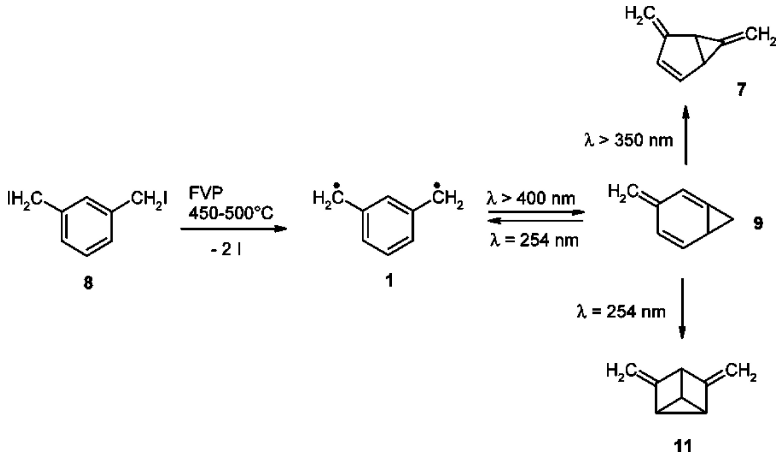

More About This Article

Additional resources and features associated with this article are available within the HTML version:

- Supporting Information
- Links to the 1 articles that cite this article, as of the time of this article download
- Access to high resolution figures
- Links to articles and content related to this article
- Copyright permission to reproduce figures and/or text from this article

View the Full Text HTML

J|A|C|S
ARTICLES
Published on Web 02/16/2008

Matrix Isolation, Spectroscopic Characterization, and Photoisomerization of *m*-Xylylene

Patrik Neuhaus, Dirk Grote, and Wolfram Sander*

Lehrstuhl für Organische Chemie II der Ruhr-Universität, D-44780 Bochum, Germany

Received May 15, 2007; E-mail: wolfram.sander@rub.de

Abstract: A new efficient synthesis of *m*-xylylene **1** is reported. The diradical **1** was trapped in argon matrices at 10 K and characterized by IR, UV−vis, and EPR spectroscopy. The syntheses reported before only allowed generation of **1** in organic glasses, and the spectroscopic identification was limited to fluorescence and EPR spectroscopy. Diradical **1** proved to be highly photolabile, and irradiation results in the formation of three isomeric hydrocarbons **7**, **9**, and **11** which could be identified by comparison of their IR spectra with the results of DFT calculations.

Introduction

m-Xylylene **1** is the parent molecule of all high-spin polyradical systems with *meta*-phenylene coupling units used to design organic magnetic materials. A stable derivative of **1**, the tetraphenyl-substituted Schlenk's hydrocarbon, was synthesized as early as 1915.[1] In 1970 it was identified as a triplet ground state diradical by EPR spectroscopy.[2] The parent *m*-xylylene **1** has been generated by UV irradiation of *m*-xylene **2** in organic glasses, however, in very low yield with the monoradical as major radical species formed. Diradical **1** could be identified by the sensitive fluorescence spectroscopy in these experiments (Scheme 1).[3] Later it was found that the yield of **1** could be increased by using either dichloroxylene **3**[4,5] or *bis*-diazo compound **4**[6] as photochemical precursors in ethanol glasses at 77 K. An alternative synthesis of **1** is the photofragmentation of **6** to produce the highly strained hydrocarbon **7** which rapidly rearranges to **1**.[7,8] Platz et al. were able to record the EPR spectrum of **1** in organic glasses,[4,6] which proved the triplet ground state of this diradical.

The singlet−triplet gap (ΔE_{ST}) of diradical **1** was determined by Wenthold et al. using photoelectron spectroscopy to 9.6 ± 0.2 kcal/mol.[9] UB3LYP/6-31G(d) calculations predict ΔE_{ST} = 6.72 kcal/mol without and 13.2 kcal/mol with spin projection, which probably overcorrects singlet energies.[10] In a recent *ab initio* study ΔE_{ST} = 13.8 kcal/mol was obtained.[11,12] The heat of formation of **1** was determined by gas-phase ion chemistry

Scheme 1. Synthesis of *m*-Xylylene **1**

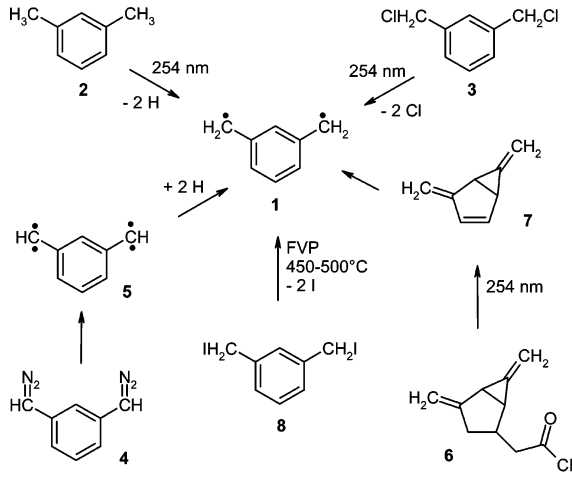

to 80.8 kcal/mol,[13] ca. 33 kcal/mol higher than the quinoid *ortho*- and *para*-xylylene. The first and second bond dissociation energies (BDE) of *m*-xylene **2** to give **1** via the monoradical were measured to 90.1 and 90.7 kcal/mol, respectively, with errors of 2−3 kcal/mol.[13] DFT calculations predict BDEs of 87.6 and 85.6 kcal/mol, which are within the error limits of the experiment. The slightly smaller second BDE suggests a small stabilizing interaction between the radical centers.[14]

All the syntheses of **1** reported so far (Scheme 1) are based on UV photolysis of suitable precursors. However, as shown here, diradical **1** is highly photolabile, and therefore its yield is diminished by secondary photolysis. Only small amounts of **1** survive in photostationary equilibria, and high yields of **1** can only be obtained if photochemical steps are avoided in its synthesis.

Results and Discussion

***m*-Xylylene 1.** Flash vacuum pyrolysis (FVP) of 1,3-*bis*-iodomethyl-benzene **8** at 400 °C and subsequent trapping of

(1) Schlenk, W.; Brauns, M. *Ber. Chem. Ges.* **1915**, *48*, 661−669.
(2) Kothe, G.; Denkel, K. H.; Suemmermann, W. *Angew. Chem., Int. Ed. Engl.* **1970**, *9*, 906−907.
(3) Migirdicyan, E.; Baudet, J. *J. Am. Chem. Soc.* **1975**, *97*, 7400−7404.
(4) Haider, K.; Platz, M. S.; Despres, A.; Lejeune, V.; Migirdicyan, E.; Bally, T.; Haselbach, E. *J. Am. Chem. Soc.* **1988**, *110*, 2318−2320.
(5) Haider, K. W.; Migirdicyan, E.; Platz, M. S.; Soundararajan, N.; Despres, A. *J. Am. Chem. Soc.* **1990**, *112*, 733−738.
(6) Wright, B. B.; Platz, M. S. *J. Am. Chem. Soc.* **1983**, *105*, 628−630.
(7) Goodman, J. L.; Berson, J. A. *J. Am. Chem. Soc.* **1984**, *106*, 1867−1868.
(8) Goodman, J. L.; Berson, J. A. *J. Am. Chem. Soc.* **1985**, *107*, 5409−5424.
(9) Wenthold, P. G.; Kim, J. B.; Lineberger, W. C. *J. Am. Chem. Soc.* **1997**, *119*, 1354−1359.
(10) Zhang, G.; Li, S.; Jiang, Y. *J. Phys. Chem. A* **2003**, *107*, 5573−5582.
(11) Wang, T.; Krylov, Anna, I. *J. Chem. Phys.* **2005**, *123*, 104304.
(12) Wang, T.; Krylov, A. I. *Chem. Phys. Lett.* **2006**, *425*, 196−200.
(13) Hammad, L. A.; Wenthold, P. G. *J. Am. Chem. Soc.* **2000**, *122*, 11203−11211.
(14) Zhang, D. Y.; Borden, W. T. *J. Org. Chem.* **2002**, *67*, 3989−3995.

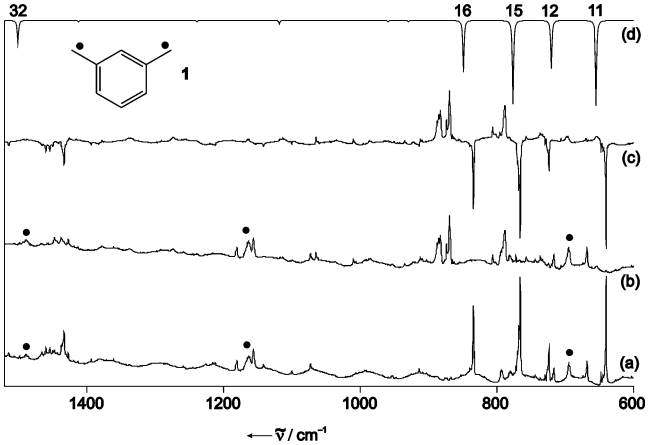

Figure 1. IR spectra showing the synthesis and the photochemistry of *m*-xylylene **1** in argon at 10 K. (a) FVP of 1,3-*bis*-iodomethyl-benzene **8** at 450 °C and trapping the products in argon at 10 K. Black dots indicate remaining **8**. (b) Same matrix after $\lambda > 400$ nm irradiation. (c) Difference IR spectrum (b) − (a). (c) IR spectrum of **1** calculated at the UB3LYP/6-311G(d,p) level of theory.

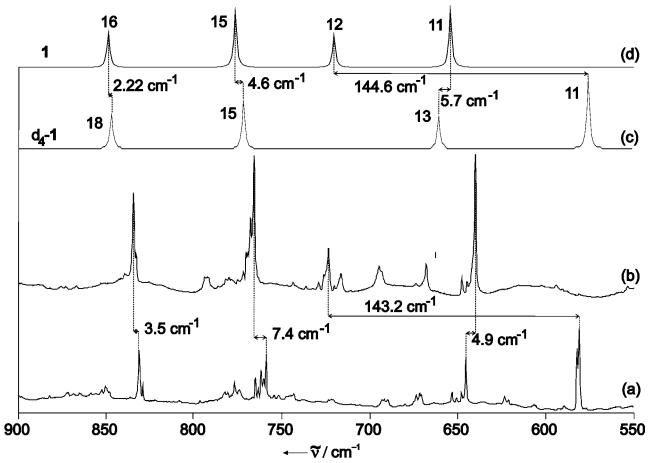

Figure 2. IR spectra in the range 550−900 cm^{-1} of *m*-xylylene **1** and its tetradeuterated isotopomer d_4-**1** showing isotopic shifts of the out-of-plane deformation modes. (a) d_4-**1** in Ar at 10 K. (b) **1** in Ar at 10 K. (c) UB3LYP/6-311G(d,p) calculated IR spectrum of d_4-**1**. (d) UB3LYP/6-311G(d,p) calculated IR spectrum of **1**.

the products in argon at 10 K result in a marked decrease of precursor **8** and formation of a new product **1**. The newly formed product **1** shows strong IR absorptions at 1434, 835, 766, 724, and 641 cm^{-1} (Figure 1, Table 1). At 450 °C, the highest yield of **1** is obtained, whereas above 500 °C further products are formed and the amount of **1** decreases. By comparison of the experimental IR data with calculations at the UB3LYP level of theory compound **1** was assigned the structure of *m*-xylylene. Traces of **1** were also formed on direct UV irradiation of matrix-isolated **8**. However, due to the photolability of **1** this is a highly inefficient process.

The four strong vibrations of **1** between 835 and 641 cm^{-1} are assigned to B_1 symmetrical o.o.p. C−H deformation vibrations and the absorption at 1434 cm^{-1} to a B_2 symmetrical combination of C−C stretching and i.p. C−H deformation vibration. For the B_2 symmetrical mode a frequency of 1500 ± 40 cm^{-1} was previously determined from photoelectron spectroscopy in the gas phase.[9] Deuteration of the benzylic positions in d_4-**1** leads to characteristic isotopic shifts, again in excellent agreement with the calculated values (Figure 2, Table 1). The largest red-shift of 143.2 cm^{-1} (calculated 144.6 cm^{-1}) is found for the vibration at 724 cm^{-1}, indicating a large contribution of the benzylic H atoms. The other three B_1 vibrations are characterized as benzene C−H o.o.p. deformation vibrations and consequently show only small isotopic shifts (3−8 cm^{-1}) in d_4-**1**. For the C−H stretching vibrations involving the benzylic hydrogen atoms also large isotopic shifts are predicted; however, these vibrations are overlapping with bands of the precursor, secondary products, and contaminations and are thus difficult to assign.

The symmetry of the strongest IR bands of **1** was determined by measuring the IR dichroism of partially oriented matrices. This method depends on the partial bleaching of a matrix-isolated compound with linear polarized light. Diradical **1** is photolabile toward 400 nm irradiation (see below), and linear polarized light of this wavelength was used for the photoselection experiments. The molecules of **1** are initially randomly oriented in the matrix. Molecules with their electronic transition moments oriented parallel to the E vector of the polarized light will show a more efficient photochemistry than those with a perpendicular orientation. The result is a photoselection of both

Table 1. IR Spectroscopic Data of *m*-Xylylene **1** and d_4-**1**

mode no.	sym.	$\tilde{\nu}_{exp}$/cm^{-1} ($I_{exp,rel}$)[a]	$\tilde{\nu}_{calc}$/cm^{-1} ($I_{calc,rel}$)[b]	$\tilde{\nu}_{exp}$/cm^{-1} ($I_{exp,rel}$)[a]	$\tilde{\nu}_{calc}$/cm^{-1} ($I_{calc,rel}$)[b]	assignment	pol.
				d_4	**d_4**		
11	B_1	640.5 (100)	655.0 (97)	645.6 (45)	661.3 (45)	$C^{2,4,6}$—H out-of-plane deformation	−
12	B_1	723.9 (45)	721.0 (55)	581.0 (100)	576.5 (97)	$C^{7,8}$—H_2 out-of-plane wagging	−
15	B_1	766.4 (90)	777.0 (95)	759.1 (65)	772.6 (67)	$C^{2,4,5,6}$—H out-of-plane deformation	−
16	B_1	834.9 (60)	849.0 (59)	831.4 (50)	847.3 (50)	C^{2}—H out-of-plane deformation	−
32	B_2	1433.9 (25)	1502.0 (25)	1459.8 (15)	1488.5 (17)	$C^{7,8}$—H_2 rocking; C═C aromatic stretching; $C^{2,4,5,6}$—H in-plane deformation	+
35	A_1	*d*	3144.6 (2)	2214.4 (15)	2283.6 (2)	symmetric $C^{7,8}$—H_2 stretching	*d*
36	B_2	3034.4 (−)[c]	3145.1 (23)	2214.4 (15)	2283.9 (12)	symmetric $C^{7,8}$—H_2 stretching	*d*
41	B_2	3110.6 (−)[c]	3240.9 (8)	2347.3 (15)	2415.7 (5)	asymmetric $C^{7,8}$—H_2 stretching	*d*
42	A_1	3114.2 (−)[c]	3241.1 (7)	2347.3 (15)	2416.0 (17)	asymmetric $C^{7,8}$—H_2 stretching	*d*

[a] Argon, 10 K. [b] UB3LYP/6-311G(d,p). [c] Intensity is not assigned due to the broad peaks in this region. [d] Not assigned.

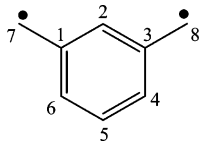

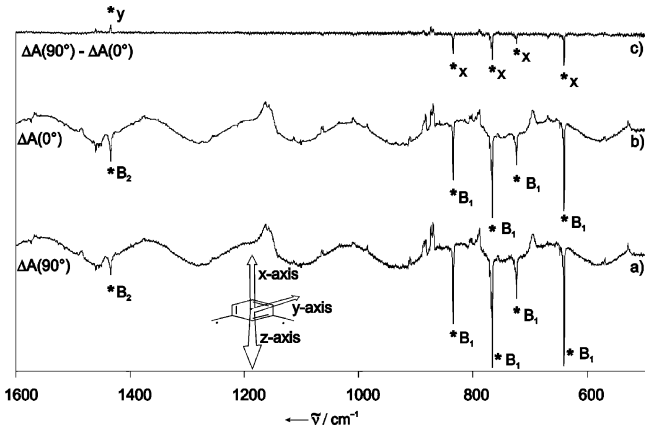

Figure 3. IR dichroism of **1** in argon at 10 K after partial photolysis of **1** using linearly polarized visible light (400−450 nm). The IR bands assigned to **1** are marked with stars. (a) Difference IR spectrum with the IR polarization filter perpendicular to the polarization direction of the photolysis (90° between IR and vis light polarization). Peaks pointing downward decrease and peaks pointing upward increase during irradiation. (b) Difference IR spectrum with the IR polarization filter parallel to the polarization direction of the photolysis (0° between IR and vis light polarization). Peaks pointing downward decrease upon irradiation, and peaks pointing upward increase during irradiation. B_1 and B_2 indicate the symmetry of the vibrations. (c) Difference spectrum between (a) and (b) showing differences in the polarization directions of IR bands. Since this effect is small, only strong absorptions can be observed.

1 and the products with respect to E.[15,16] Since the symmetry of **1** is C_{2v}, the transition moment of the electronic excitation as well as the vibrational transition moments have to be parallel to the principal axes *x*, *y*, or *z* of the molecule. Since the orientation is uniaxial, only two distinct polarization orientations are possible (parallel or perpendicular to this axis, the two perpendicular axes are undistinguishable in these experiments). This is found in the experiment (Figure 3): the out-of-plane deformation vibrations of B_1 symmetry are polarized perpendicular to the B_2 symmetrical in-plane deformation vibration. The transition moments of the B_1 vibrations are oriented parallel to the *z* axes, whereas that of B_2 is parallel to *x*. This clearly demonstrates the C_{2v} symmetry of **1** and confirms the assignment of the five strongest IR bands of **1**. Since the photoselection of **1** is low and the effect is very small, the polarization direction of the weaker bands could not be determined.

The UV−vis spectrum of matrix-isolated **1** shows transitions at 231 nm (strong, broad), 279 nm (weak), 287 nm (strong, sharp), and 433 nm (very weak, Figure 4). The 279 and 287 nm absorptions (presumably one electronic transition with a vibrational progression) are similar to the transitions observed in a fluorescence excitation spectrum (ca. 295 and 287 nm).[3] We could not verify an additional transition at 312 nm described in this paper. The very weak transition at 433 nm is in accordance with the observation of fluorescence on excitation of **1** at 439 nm.[17] The strong and broad absorption with a maximum at 231 nm has not been described in literature, thus far.

The EPR spectrum of **1**, matrix-isolated in argon at 4 K, showed a very intense triplet signal with zfs parameters $|D/hc| = 0.011$ cm^{-1} and $|E/hc| = 0.001$ cm^{-1} (Figure 5), in excellent agreement with the published values.[6] In addition, a low-intensity half field signal, characteristic of triplet EPR spectra, was found at 1708 G. This clearly demonstrates that indeed a triplet state is observed.

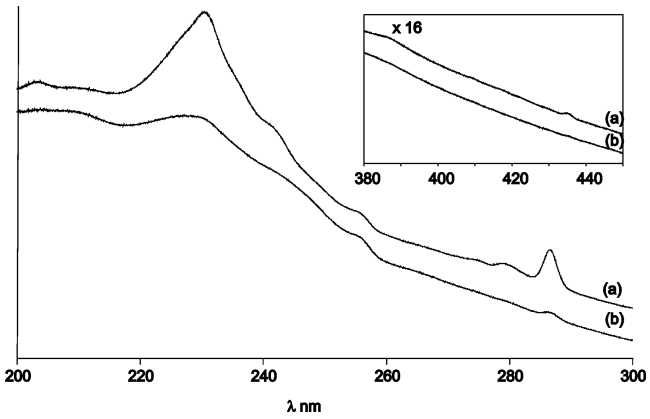

Figure 4. (a) UV−vis spectrum of an Ar matrix containing the FVP products of 1,3-*bis*-iodomethyl-benzene **8**. (b) UV−vis spectrum of the same matrix after irradiation with $\lambda = 400-450$ nm. Inset: 380−450 nm.

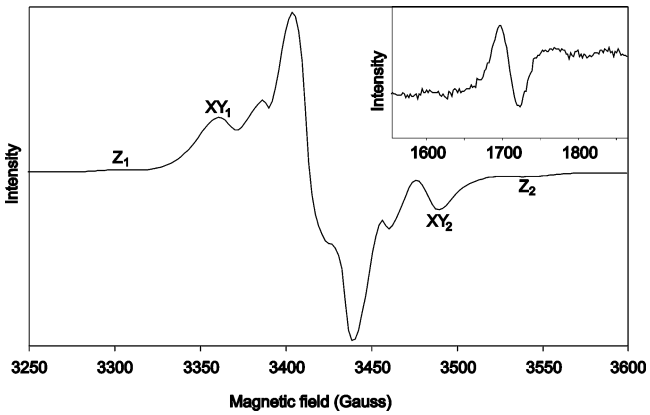

Figure 5. EPR spectrum obtained after FVP of 1,3-*bis*-iodomethyl-benzene **8** at 450 °C and trapping the products in argon at 4 K. Inset: half-field signal.

Photochemistry of 1. Irradiation of matrix-isolated **1** with visible light ($\lambda > 400$ nm) results in a decrease of all IR, UV−vis, and EPR bands assigned to **1** and formation of the two new C_8H_8 isomers 4,6-dimethylene-bicyclo[3.1.0]hex-2-ene **7** and 3-methylene-bicyclo[4.1.0]hepta-1,4-diene **9** (Scheme 2). Irradiation at a slightly shorter wavelength ($\lambda > 350$ nm) results in the rearrangement of **9** to **7** (Figure 6), while short wavelength UV irradiation ($\lambda = 254$ nm) leads partially back to diradical **1** and partially to the formation of a further isomer, 3,5-dimethylene-tricyclo[2.2.0.0*2,6*]hexane **11**. The reversible photochemistry (Figures 6−8) demonstrates that **7**, **9**, and **11** are C_8H_8 isomers of **1** formed in photostationary equilibria. Since the equilibrium between these species depends on the irradiation conditions, sets of IR bands can be assigned to each isomer, and the comparison with the results of DFT calculations allows the identification of the compounds.

Hydrocarbon **7** shows characteristic C═C stretching vibrations of the two *exo*-methylene groups at 1745.3 cm^{-1} (C(6)═C(8)) and 1640.6 cm^{-1} (C(4)═C(7)) with deuterium shifts of 18.9 and 26.2 cm^{-1}, respectively, in d_4-**7** (Figure 6, Table 2). The high frequency of the former vibration is characteristic of

(15) Thulstrup, E. W.; Michl, J. *Elementary Polarization Spectroscopy*; VCH: New York, NY 1989.
(16) Michl, J., Thulstrup, E. W., Eds. *Spectroscopy with Polarized Light: Solute Alignment by Photoselection, Liquid Crystals, Polymers, and Membranes*; VCH: Weinheim, 1995.
(17) LeJeune, V.; Despres, A.; Migirdicyan, E. *J. Phys. Chem.* **1984**, *88*, 2719−2722.

Scheme 2. Photochemistry of *m*-Xylylene **1**

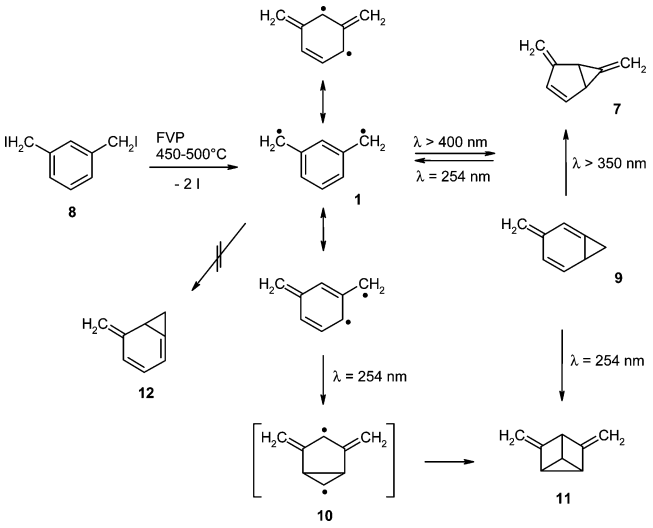

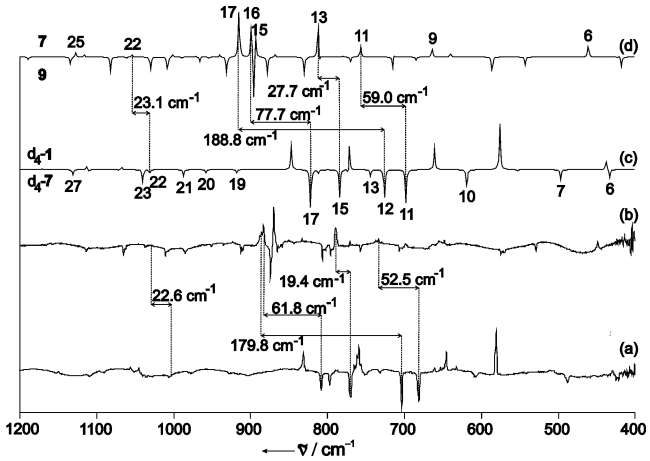

Figure 6. Difference IR spectra showing the photochemical interconversion of **1**, **7**, and **9** in argon at 10 K. The experimental difference spectra are compared to simulated difference spectra based on calculations at the B3LYP/6-311G(d,p) level of theory. (a) $\lambda = 254$ nm irradiation converts d_4-**7** (disappearing, peaks pointing downward) into d_4-**1** (appearing, peaks pointing upward). (b) $\lambda > 350$ nm irradiation converts **9** (disappearing, peaks pointing downward) into **7** (appearing, peaks pointing upward). (c) Simulated difference spectrum d_4-**1**−d_4-**7** corresponding to (a). (d) Simulated difference spectrum **7**−**9** corresponding to (b). The isotopic shifts of the *exo*-methylene groups of **7** are shown in the spectra.

methylenecyclopropanes, and the isotopic shifts demonstrate that both *exo*-methylene groups are deuterated in d_4-**7**. Other intense IR absorptions are found in the fingerprint region of the spectrum. The most intense band at 883.2 cm^{-1} shows a very large isotopic shift of 179.8 cm^{-1} and is assigned to the C(8)-H_2 out-of-plane wagging deformation. The band positions, relative intensities, and isotopic shifts are nicely reproduced by DFT calculations, as can be seen by the very similar patterns of the simulated (from DFT calculations) and experimental difference IR spectra (Figure 6).

The strongest IR absorption of hydrocarbon **9** is (like in **7**) the C(8)H_2 out-of-plane wagging vibration of the *exo*-methylene group at 874.2 cm^{-1}, in good agreement with the calculation (Figure 7, Table 3). As expected, in d_4-**9** this band shows a very large isotopic shift (110.7 cm^{-1}). Another band with a large

Table 2. IR Spectroscopic Data of **7** and d_4-**7**

mode no.	$\tilde{\nu}_{exp}$/cm^{-1} ($I_{exp,rel}$)[a]	$\tilde{\nu}_{calc}$/cm^{-1} ($I_{calc,rel}$)[b]	$\tilde{\nu}_{exp}$/cm^{-1} ($I_{exp,rel}$)[a]	$\tilde{\nu}_{calc}$/cm^{-1} ($I_{calc,rel}$)[b]	assignment
			d_4	**d_4**	
6	448.8 (25)	461.8 (23)	424.8 (20)	433.1 (18)	C^1—C^6—C^8 deformation
7	—[c]	605.4 (0)	487.7 (20)	497.4 (22)	$C^{7,8}$—H_2 twisting; in-plane ring deformation
8	628.0 (5)	640.3 (7)	607.5 (25)	619.5 (33)	skeletal vibration
11	733.6 (20)	757.8 (23)	681.1 (75)	698.8 (70)	asymmetric H—C^1—C^5—H bending; out-of-plane ring deformation
12	—[c]	780.4 (2)	731.7 (15)	744.9 (14)	asymmetric H—C^1—C^5—H bending; in-plane ring deformation
13	789.7 (80)	812.5 (84)	770.3 (65)	784.8 (59)	H—C^2═C^3—H out-of-plane deformation; C^8—H_2 twisting
14	855.5 (2)	868.7 (5)	—[c]	851.9 (0)	asymmetric H—C^1—C^5—H bending
15	869.9	893.2 (51)	797.1 (25)	813.0 (7)	C^8—H_2 twisting; C^7—H_2 out-of-plane wagging
16	869.9 (110)	899.9 (69)	808.1 (45)	822.2 (81)	C^8—H_2 twisting; C^7—H_2 out-of-plane wagging
17	883.2 (100)	915.3 (100)	703.4 (60)	726.5 (59)	C^8—H_2 out-of-plane wagging
18	923.3 (5)	941.0 (5)	797.1 (25)	813.0 (7)	C^7—H_2 in-plane rocking
22	1029.1 (5)	1054.2 (5)	1006.5 (5)	1031.1 (7)	$C^{1,5}$—H bending
24	—[c]	1117.0 (5)	1036.0 (10)	1040.9 (25)	asymmetric H—C^2═C^3—H in plane deformation; C^7—H_2 rocking
25	1099.6 (10)	1127.3 (10)	1109.5 (10)	1131.4 (11)	asymmetric H—C^2═C^3—H in plane deformation; C^7—H_2 rocking
29	1336.2 (10)	1358.8 (15)	1341.2 (20)	1364.5 (18)	symmetric H—C^2═C^3—H in plane deformation; C^7—H_2 bending
32	1565.3 (5)	1620.7 (7)	1573.0 (10)	1615.2 (14)	C^2═C^3 stretching
33	1640.6 (80)	1696.4 (76)	1614.4 (70)	1658.8 (100)	C^4═C^7 stretching
34	1745.3 (40)	1817.1 (41)	1726.4 (50)	1783.7 (66)	C^6═C^8 stretching

[a] Argon, 10 K. [b] B3LYP/6-311G(d,p). [c] Not assigned.

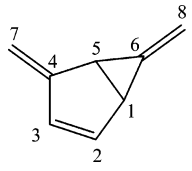

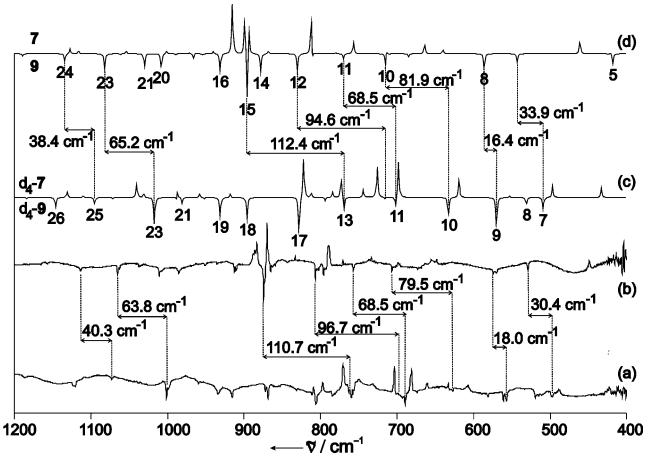

Figure 7. Difference IR spectra showing the photochemical interconversion of **7** and **9** in argon at 10 K. The experimental difference spectra are compared to simulated difference spectra based on calculations at the B3LYP/6-311G(d,p) level of theory. (a) $\lambda > 350$ nm irradiation converts d_4-**9** (disappearing, peaks pointing downward) into d_4-**7** (appearing, peaks pointing upward). (b) $\lambda > 350$ nm irradiation converts **9** (disappearing, peaks pointing downward) into **7** (appearing, peaks pointing upward). (c) Simulated difference spectrum d_4-**7**−d_4-**9** corresponding to (a). (d) Simulated difference spectrum **7**−**9** corresponding to (b). The isotopic shifts of the *exo*-methylene groups of **9** are shown in the spectra.

isotopic shift is the C(7)H_2 twisting vibration at the cyclopropane ring at 796.0 cm^{-1} (96.7 cm^{-1} isotopic shift in d_4-**9**). The strongly distorted bridgehead double bond C(1)═C(2) is part of a methylenecyclopropane unit. Consequently, the C(1)═C(2) stretching vibration is found at very high frequency (1753.6 cm^{-1}). Since no deuterium atoms are directly attached to this double bond in d_4-**9** the isotopic shift is small.

The third isomer formed during the photolysis of **1** is the tricyclic hydrocarbon **11**. Due to its higher symmetry the IR spectrum of **11** is simpler than that of **7** and **9** (Figure 8, Table 4). The strongest absorptions are the antisymmetrical and symmetrical combinations of the two *exo*-methylene C═C stretching vibrations at 1678.6 (16.0 cm^{-1} isotopic shift) and 1683.8 cm^{-1} (14.6 cm^{-1} isotopic shift), respectively. The antisymmetrical and symmetrical combinations of the wagging vibrations of the *exo*-methylene groups are found at 851.7 (64.5 cm^{-1} isotopic shift) and 852.9 cm^{-1} (63.1 cm^{-1} isotopic shift), respectively. As with **7** and **9** the IR spectrum of **11** is very nicely reproduced by DFT calculations. There is no evidence for the formation of further isomeric hydrocarbons such as **12** (Figure 9, Scheme 2).

All three isomers **7**, **9**, and **11** contain a fused three-membered ring resulting in high strain energy which pushes their energy well above that of T-**1** and even S-**1**. The most stable of the three isomers is **7** which at the B3LYP/6-311G(d,p) level of theory is calculated to be 19.2 kcal/mol above T-**1** and 13 kcal/mol above S-**1**. The hydrocarbon **9** with an *anti*-Bredt bridgehead double bond is with 25.7 kcal/mol relative to T-**1** even less stable (Table 5). In **11** the three-membered ring is fused to

Table 3. IR Spectroscopic Data of **9** and **9**-d_4

mode no.	$\tilde{\nu}_{exp}$/cm^{-1} ($I_{exp,rel}$)[a]	$\tilde{\nu}_{calc}$/cm^{-1} ($I_{calc,rel}$)[b]	$\tilde{\nu}_{exp}$/cm^{-1} ($I_{exp,rel}$)[a]	$\tilde{\nu}_{calc}$/cm^{-1} ($I_{calc,rel}$)[b]	assignment
			d_4	**d_4**	
7	528.9 (20)	543.6 (18)	498.5 (30)	509.7 (22)	in-plane ring deformation; C^7—H_2 twisting
8	575.0 (30)	586.7 (28)	557.0 (75)	570.3 (51)	skeletal vibration
10	706.6 (25)	715.8 (31)	627.1 (25)	633.9 (32)	C^7—H_2 twisting; ring deformation
11	757.4 (15)	770.8 (10)	689.7 (30)	702.3 (19)	C^5—H bending; C^8—H_2 twisting; in-plane ring deformation
12	796.0 (30)	811.1 (42)	699.3 (1)	716.5 (3)	symmetric H—C^4═C^5—H out-of-plane deformation; C^7—H_2 twisting
13	806.6 (35)	830.2 (36)	−[c]	769.3 (25)	C^2—H bending; C^7—H_2 rocking; C^8—H_2 twisting
15	874.2 (100)	896.6 (100)	763.5 (100)	784.2 (48)	C^8—H_2 out-of-plane wagging
14?			806.1 (80)	828.6 (64)	C^7—H_2 twisting; C^1—C^6—C^5 deformation
16	912.6 (30)	931.2 (34)	868.5 (75)	896.4 (41)	$C^{2,6}$—H bending; C^7—H_2 twisting; C^3—C^4—C^5 deformation
20	985.1 (30)	1009.0 (26)	−[c]	988.7 (9)	C^7—H_2 wagging; C^2—C^1—C^7 deformation
23	1065.2 (35)	1082.7 (31)	1001.4 (80)	1017.5 (51)	C^7—H_2 rocking; C^6—H bending
24	1113.4 (10)	1134.4 (15)	1073.1 (15)	1096.0 (12)	C^6—H bending; asymmetric H−C^4═C^5−H in-plane deformation
25	1157.1 (5)	1189.0 (5)	−[c]	1184.6 (3)	asymmetric H−C^4═C^5—H in-plane deformation; C^2—H bending
26	1256.4 (1)	1281.9 (2)	−[c]	1271.7 (0)	$C^{2,6}$—H bending
29	1378.0 (10)	1399.6 (15)	1378.9 (25)	1402.0 (12)	H−C^4═C^5—H in-plane deformation
32	1567.2 (10)	1622.2 (13)	1541.2 (35)	1595.3 (32)	C^4═C^5 stretching; C^3═C^8 stretching
33	1612.9 (15)	1671.2 (39)	1599.6 (25)	1650.0 (19)	C^3═C^8 stretching; C^4═C^5 stretching
34	1753.6 (20)	1768.7 (10)	−[c]	1765.0 (16)	C^1═C^2 stretching
36	−[c]	3096.5 (78)	2211.1 (15)	2247.1 (38)	symmetric C^7—H_2 stretching
41	−[c]	3180.1 (39)	2313.7 (25)	2369.8 (25)	asymmetric C^7—H_2 stretching
42	−[c]	3220.5 (28)	2330.7 (25)	2399.4 (16)	asymmetric C^8—H_2 stretching

[a] Argon, 10 K. [b] B3LYP/6-311G(d,p). [c] Not assigned.

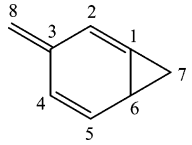

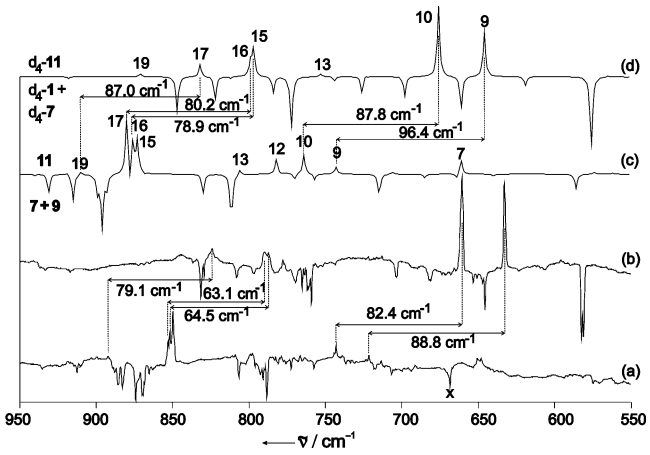

Figure 8. Difference IR spectra showing the photochemical interconversion of **1**, **7**, **9**, and **11** in argon at 10 K. The experimental difference spectra are compared to simulated difference spectra based on calculations at the B3LYP/6-311G(d,p) level of theory. (a) $\lambda > 320$ nm irradiation converts a mixture of **7** and **9** (disappearing, peaks pointing downward) into **11** (appearing, peaks pointing upward). (b) $\lambda > 260$ nm irradiation converts a mixture of d_4-**1** and d_4-**7** (disappearing, peaks pointing downward) into d_4-**11** (appearing, peaks pointing upward). (c) Simulated difference spectrum (**7** + **9**) − **11** corresponding to (a). (d) Simulated difference spectrum (d_4-**1** + d_4-**7**) − d_4-**11** corresponding to (b). The isotopic shifts of the *exo*-methylene groups of **11** are shown in the spectra.

two four-membered rings resulting in a relative energy of 48.6 kcal/mol. Thus, even from S-**1** the ring-closure to give **7**, **9**, or **11** is highly endothermic and thus requires photochemical excitation in addition to populate the singlet state from the triplet ground state.

The hydrocarbons **7**, **9**, and **11** show the same CH- and CC-connectivity as diradical **1**. Formally, the rearrangement of **1** to **7** requires the formation of one new bond between C(2) and C(6) in diradical **1**, and that of **9** requires the formation of one new bond between C(2) and C(7). In **1** these carbon atoms bear high spin density as can be deduced from the corresponding resonance structures (Scheme 2). The formation of **11** requires the formation of two new bonds: one between C(2) and C(5) and the other between C(4) and C(6). A diradical such as **10** could be an intermediate; however, there is no evidence for this in our experiments.

Conclusion

The synthesis of **1** via FVP of **8** has a number of advantages compared to the previously known photochemical routes: (i) up-scaling to obtain preparative amounts of **1** is easily possible, (ii) no photochemical step is necessary that reduces the yield of the photolabile **1**, and (iii) the diradical **1** can be trapped in inert gas matrices without the formation of close radical pairs. The formation of radical pairs is unavoidable if a matrix-isolated photochemical precursor is irradiated. Annealing of these matrices rapidly leads back to the starting material via radical recombination, and thus other intermolecular reactions occur, if at all, in very low yields. In contrast, the synthesis via FVP allows us to investigate the chemistry of **1** both in matrices and via classical trapping experiments.

It is interesting to compare the high yield of diradical **1** obtained by the FVP of **8** with the similar synthesis of *meta*-benzyne from 1,3-diiodobenzene.[18−20] The synthesis of the less stable *meta*-benzyne requires much higher FVP temperatures and produces only very low yields of the benzyne, while the generation of the related 3,5-pyridyne is more successful.[21] The photochemical generation of matrix-isolated radicals via photolysis of C−I bonds depends in a nonpredictable way on the matrix (sometimes argon, sometimes neon gives better yields), on the matrix temperature (4 K or 10 K), and the nature of the precursor.[22,23] It is thus not surprising that the photolysis of matrix-isolated **8** produces only very low yields of **1** which in addition is diminished by rearrangement to **7**, **9**, and **11**.

The clean thermal synthesis of **1** allows a thorough spectroscopic characterization of this diradical. A detailed IR spectroscopic investigation including isotopic substitution and determination of the IR dichroism of the strongest bands is in accordance with the expected C_{2v}-symmetrical structure of **1**. The EPR and UV−vis spectra are in agreement with previously reported spectroscopic data.

Table 4. IR Spectroscopic Data of **11** and d_4-**11**

vib. no.	symmetry	$\tilde{\nu}_{exp}$/cm^{-1} ($I_{exp,rel}$)[a]	$\tilde{\nu}_{calc}$/cm^{-1} ($I_{calc,rel}$)[b]	$\tilde{\nu}_{exp}$/cm^{-1} ($I_{exp,rel}$)[a]	$\tilde{\nu}_{calc}$/cm^{-1} ($I_{calc,rel}$)[b]	assignment
				d$_4$	**d$_4$**	
9	A″	721.6 (5)	743.0 (7)	632.8 (40)	646.6 (32)	$C^{7,8}$—H_2 twisting
10	A′	742.9 (30)	764.2 (19)	660.5 (60)	676.4 (51)	C^7—C^3—C^4 and C^4—C^5—C^8 out-of-plane deformation; C^4—H bending
12	A″	763.8 (25)	782.4 (14)	−[c]	771.8 (1)	$C^{1,2,6}$—H bending
13	A′	784.5 (1)	806.6 (5)	−[c]	753.5 (2)	$C^{2,6}$—H bending
16	A″	851.7 (60)	876.4 (30)	787.2 (15)	797.5 (19)	$C^{7,8}$—H_2 wagging
17	A′	852.9 (40)	880.1 (54)	789.8 (15)	799.9 (11)	$C^{7,8}$—H_2 wagging
18	A″	899.7 (1)	910.8 (3)	867.1 (1)	871.0 (2)	$C^{7,8}$—H_2 rocking; C^4—H bending
19	A′	903.2 (1)	919.5 (2)	824.1 (10)	832.5 (9)	$C^{7,8}$—H_2 rocking;
20	A″	−[c]	994.7 (3)	940.9 (10)	957.5 (8)	$C^{1,2,6}$—H deformation; $C^{7,8}$—H_2 twisting
24	A′	1092.2 (1)	1117.8 (5)	1069.0 (1)	1085.2 (1)	$C^{1,4}$—H bending
28	A′	1237.4 (1)	1259.3 (5)	1211.7 (10)	1229.7 (7)	$C^{1,2,6}$—H bending; $C^{7,8}$—H_2 rocking
33	A″	1678.6 (60)	1747.1 (98)	1662.6 (60)	1709.7 (98)	C^3═C^7 and C^5═C^8 stretching
34	A′	1683.8 (100)	1758.7 (69)	1669.2 (100)	1719.9 (70)	C^3═C^7 and C^5═C^8 stretching

[a] Argon, 10 K. [b] B3LYP/6-311G(d,p). [c] Not assigned.

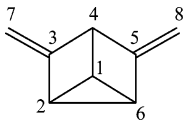

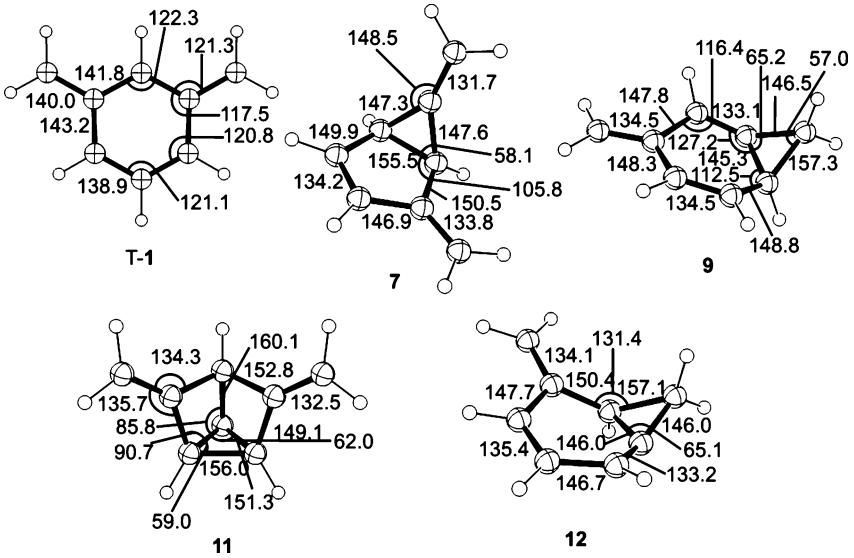

Figure 9. (U)B3LYP optimized geometries of T-**1**, **7**, **9**, **11** and **12**. Bond length is given in pm, and bond angle, in deg.

Table 5. DFT Energies of the C_8H_8 Isomers

molecule	$(E + ZPC)^a$ hartrees	E_{rel}, kcal/mol
T-**1**[b]	−309.534386	0
S-**1**[b]	−309.524472	6.22
7[c]	−309.503791	19.20
9[c]	−309.493361	25.74
11[c]	−309.456873	48.64
12[c]	−309.491230	27.08

[a] All energies including zero-point vibrational energy correction (ZPC) without spin-projection. [b]UB3LYP/6-311G(d,p). [c]B3LYP/6-311G(d,p).

Experimental Section

1,3-*Bis*-iodomethyl-benzene 8. Compound **8** was synthesized according to a literature procedure.[24]

1,3-*Bis*-(hydroxymethyl)-benzene-d_4. To a refluxing and stirred suspension of lithiumaluminiumdeuterid LAD (0.60 g, 14.3 mmol) in anhydrous THF (20 mL) under argon a solution of dimethyl benzene-1,3-dicarboxylate (1.29 g, 6.65 mmol) in 10 mL of anhydrous THF was added dropwise. The mixture was refluxed for 5 h and cooled with ice. The excess LAD was hydrolyzed by careful addition of water (2 mL), 15% aq. NaOH (2 mL), and again water (5 mL). After stirring overnight, the white solid was filtered off and washed with several portions of THF. All organic extracts were combined, and the solvent was removed in vacuum to give a colorless oil which solidified rapidly. The crude product was used without further purification in the next step. Yield: 85%. IR (KBr) 3214, 2213, 2090, 1432, 1266, 1187, 1107, 1082, 1059, 954, 723, 690 cm^{-1}; mass spectrum, *m*/*z* 142 (M^+).

1,3-*Bis*-bromomethyl-benzene-d_4. To a stirred solution of 0.90 g (6.33 mmol) 1,3-*bis*-hydroxymethyl-benzene-d_4 in 30 mL of anhydrous THF a solution of 0.77 mL (2.23 g, 8.23 mmol) phosphorus tribromide in 15 mL of dry ether was added dropwise and stirred for 4 h at room temperature. 30 mL of water were added, and the organic layer was washed two times with 15 mL of water. After drying of the organic layer over $MgSO_4$ and evaporation of the solvent, a colorless oil was obtained which was purified by column chromatography (dichloromethane/hexane, 1:1). Yield: 75%. IR (KBr) 2274, 2179, 1483, 1427, 1186, 1064, 953, 867, 791, 694 cm^{-1}; mass spectrum, *m*/*e* 268 (M^+).

1,3-*Bis*-iodomethyl-benzene-d_4. 0.106 g (0.40 mmol) of 1,3-*bis*-bromomethyl-benzene-d_4 was dissolved in 10 mL of dry acetone, and 0.6 g of NaI (4.0 mmol) was added. After stirring under reflux for 12 h the solvent was removed, 150 mL of dichloromethane were added, and the precipitate was filtered off. Removal of the solvent under reduced pressure gave 1,3-*bis*-iodomethyl-benzene-d_4 d_4-**8**, which was further purified by column chromatography using dichloromethane and hexane (1:2) as eluent. Yield: 80%. IR (KBr) 2174, 1581, 1480, 1426, 1183, 1058, 926, 851,783, 690, 505 cm^{-1}; mass spectrum, *m*/*z* 362 (M^+).

Matrix Isolation. Matrix isolation experiments were performed by standard techniques[25] using a closed cycle helium cryostat and a CsI spectroscopic window cooled to 10 K. FTIR spectra were recorded with a standard resolution of 0.5 cm^{-1}, using a N_2(l)-cooled MCT detector in the range 400−4000 cm^{-1}. X-band EPR spectra were recorded from a sample deposited on an oxygen-free high-conductivity copper rod (75 mm length, 2 mm diameter) cooled with a closed cycle cryostat to 4 K. UV spectra were recorded in the spectroscopic range 500 to 200 nm with a standard resolution of 0.02 nm, using a Varian UV-vis NIR spectrophotometer from a sample deposited on a sapphire window cooled to 10 K by a closed cycle cryostat. Flash vacuum pyrolysis was carried out by slowly subliming **8** through a 7 cm quartz tube heated electrically with a tantalum wire.

Broadband irradiation was carried out with mercury high-pressure arc lamps in housings equipped with quartz optics and dichroic mirrors in combination with cutoff filters (50% transmission at the wavelength specified). For 254 nm irradiation a low-pressure mercury arc lamp was used.

Computational Methods. Optimized geometries and vibrational frequencies of all species were calculated at the B3LYP[26−28] level of theory employing the 6-311G(d,p) polarized valence-triple-ξ basis set.[29,30] Tight convergence criteria were used throughout. A spin-

(18) Sander, W. *Acc. Chem. Res.* **1999**, *32*, 669−676.
(19) Winkler, M.; Sander, W. *J. Phys. Chem. A* **2001**, *105*, 10422−10432.
(20) Wenk, H. H.; Winkler, M.; Sander, W. *Angew. Chem., Int. Ed.* **2003**, *42*, 502−528.
(21) Winkler, M.; Cakir, B.; Sander, W. *J. Am. Chem. Soc.* **2004**, *126*, 6135−6149.
(22) Wenk, H. H.; Sander, W. *Angew. Chem., Int. Ed.* **2002**, *41*, 2742−2745.
(23) Sander, W.; Winkler, M.; Cakir, B.; Grote, D.; Bettinger, H. F. *J. Org. Chem.* **2007**, *72*, 715−724.
(24) Kida, T.; Kikuzawa, A.; Higashimoto, H.; Nakatsuji, Y.; Akashi, M. *Tetrahedron* **2005**, *61*, 5763−5768.
(25) Dunkin, I. R. *Matrix-Isolation Techniques*; Oxford University Press: Oxford, U.K., 1998.
(26) Becke, A. D. *J. Chem. Phys.* **1993**, *98*, 5648−5652.
(27) Lee, C.; Yang, W.; Parr, R. G. *Phys. Rev. B: Condens. Matter* **1988**, *37*, 785−789.
(28) Miehlich, B.; Savin, A.; Stoll, H.; Preuss, H. *Chem. Phys. Lett.* **1989**, *157*, 200−206.
(29) McLean, A. D.; Chandler, G. S. *J. Chem. Phys.* **1980**, *72*, 5639−5648.
(30) Krishnan, R.; Binkley, J. S.; Seeger, R.; Pople, J. A. *J. Chem. Phys.* **1980**, *72*, 650−654.

unrestricted formalism was used for all high-spin systems and for singlet biradicals, whenever an instability[31] was observed. All DFT calculations were carried out with Gaussian 03.[32]

Acknowledgment. This work was financially supported by the Deutsche Forschungsgemeinschaft and the Fonds der Chemischen Industrie.

Supporting Information Available: Absolute energies, Cartesian coordinates of all calculated structures, and complete ref 32. This material is available free of charge via the Internet at http://pubs.acs.org.

JA073453D

(31) Bauernschmitt, R.; Ahlrichs, R. *J. Chem. Phys.* **1996**, *104*, 9047−9052.

(32) Frisch, M. J. et al. *Gaussian 03*; Gaussian, Inc.: Pittsburgh, PA, 2003.